



Performance comparison of commercial TiO₂: separation and reuse for bacterial photo-inactivation and emerging pollutants photo-degradation

Samuel Moles¹ · Pilar Valero¹ · Silvia Escuadra¹ · Rosa Mosteo¹ · Jairo Gómez² · María P. Ormad¹

Received: 10 September 2019 / Accepted: 3 December 2019 / Published online: 7 January 2020
© Springer-Verlag GmbH Germany, part of Springer Nature 2020

Abstract

This research aims to compare the disinfection and degradation effectiveness in water of a commercial suspension of nano-TiO₂ (TiO₂ Levenger) with the standard TiO₂ Degussa P25. Photo-inactivation and photo-degradation experiments were conducted with UVA-vis light. Concerning the disinfection, the effects of TiO₂ dose (0–2 g/l), water matrix, bacterium type (Gram-positive or Gram-negative), and bacterial regrowth after the photo-treatments were studied for each catalyst. The experimental results show that *Enterococcus* sp. (Gram-positive) was more resistant to the photo-treatments than *Escherichia coli* (Gram-negative) for both catalyst; however, postirradiation trends showed similar behavior for both bacteria, favoring regrowth for short-treated cells and decay for longer-treated ones. Caffeine was selected as a model substance of pharmaceuticals and personal care products. In terms of caffeine removal, the effects of TiO₂ dose (0–2 g/l) and water matrix were analyzed. Besides, the comparison between mechanical coagulation-flocculation-decantation and simple decantation of TiO₂ was carried out. The results show that simple decantation allowed the recovery of 97.5% of TiO₂ Degussa P25 and TiO₂ Levenger within 1 day of simple decantation, while applying the proposed mechanical coagulation-flocculation decantation 99.7% of recovery of both catalysts was achieved in 2 hours. Finally, the subsequent reuse of both catalysts was proved with little loss of efficiency in terms of photo-disinfection during the four cycles. Nevertheless, the standard TiO₂ Degussa P25 photo-degradation efficiency of caffeine decreases considerably as compared to commercial suspension of TiO₂ Levenger concerning the reutilization.

Keywords Inactivation · Caffeine · Wastewater treatment plant · Pharmaceuticals and personal care products · Emerging pollutants · Mechanical coagulation-flocculation-decantation

PPCP pharmaceuticals and personal care products

Highlights • TiO₂ Levenger produced similar inactivation and PPCP degradation than Degussa P25

- Mechanical CFD allowed the recovery of 99.7% of both catalysts in 2 hours
- Both catalysts were reused for four cycles with almost constant disinfection effectivity

Responsible Editor: Suresh Pillai

✉ Samuel Moles
sma@unizar.es

¹ Department of Chemical Engineering and Environmental Technologies, University of Zaragoza, 3 María de Luna Street, 50018 Zaragoza, Spain

² NILSA, Navarra Infraestructuras Locales S.A., Comunidad Foral de Navarra, Pamplona, Spain

Introduction

The presence of pathogenic microorganisms in water is an issue of special concern due to the potential risk of waterborne diseases. Bacteria, viruses, and protozoa can be naturally present in water or introduced as a result of the human activity. Consequently, microbial control is necessary in waters intended for different uses, such as human consumption or agricultural irrigation by means of the reuse of wastewater treatment plant effluents (WHO 2006; WHO 2016). Therefore, microbiological (*Escherichia coli*, intestinal nematodes, *Legionella* spp., etc.) and physical-chemical parameters (turbidity, suspended solids, nitrogen, etc.) have to be controlled and reduced if it is required because of their pathologic effects in humans (WHO 2016).

Pharmaceuticals and personal care products (PPCP) are a wide group of substances belonging to different chemical families. These compounds are used in human and veterinary

medicines. Therefore, many research works evidence the presence of PPCP in rivers, sea water, groundwater, and drinking water (Rodríguez-Gil et al. 2018). Furthermore, their potential adverse effects on human health, such as the development of antibiotic-resistant microbes in the aquatic environment (Adegoke Anthony et al. 2018) or changes on fish reproduction (Kidd et al. 2007), led to their cataloging as relevant environmental contaminants (belonging to the class of emerging contaminants) (1). Hence, there is a need for the development of viable water treatment processes that are able to degrade PPCP.

Caffeine ($C_8H_{10}N_4O_2$) is an alkaloid belonging to the methylxanthine family; it is present in legumes, leaves, and fruits of more than 60 plant species. Most caffeine is consumed for beverages such as coffee, tea, or energy drinks as a psychomotor stimulant. Caffeine is an example of PPCP detected in surface waters. It is extensively metabolized by the human liver to form three major metabolites by demethylation: 3,7-dimethylxanthine, 1,7-dimethylxanthine, and 1,3-dimethylxanthine. These are then broken down further in the liver by additional demethylation and oxidation and excreted mostly in the urine (Heckman et al. 2010). The presence of caffeine in surface waters has been reported (Heckman et al. 2010; Rodríguez-Gil et al. 2018), even at trace concentrations (ng/l to mg/l), being considered caffeine as an anthropogenic indicator of water pollution.

Different processes were applied to remove toxic and persistent PPCP, such as adsorption, biological treatments, coagulation-flocculation-decantation, ion exchange, and membrane processes. Nevertheless, conventional treatments are not able to completely remove PPCP. In the past few years, photocatalytic processes have become an interesting field of research due to its water-purifying potential. Among the numerous conventional technologies and advanced oxidation processes (AOPs) for water treatment, titanium dioxide (TiO_2) photocatalysis has gained importance during the last decade (Vitor and Vilar 2018).

TiO_2 can be applied in suspension or immobilized on a supporting surface, which allows a simple recovery from the solution; however the contact between reactants and catalysts is lower, and as a result, supported catalysts show lower yields in the same operational conditions (Van Gerven et al. 2007). When TiO_2 is in suspension, more TiO_2 surface is available for pollutant-catalyst interaction, thus increasing the efficiency of the process (Feitz et al. 2000, Gummy et al. 2006, van Grieken et al. 2010). Nevertheless, the main disadvantage of this process in terms of economic viability is the need to recover the suspended TiO_2 after the treatment (Malato et al. 2009). Several technologies have been studied for TiO_2 separation, including decantation (Keller et al. 2010, Hsiung et al. 2016) and membrane filtration (Ollis 2003, Augugliaro et al. 2006), but associated problems, such

as low decantation rates or membrane fouling, respectively, are often reported. Regardless of the way of application, reuse of TiO_2 has been successfully implemented for several cycles showing little or negligible deactivation in methylene blue degradation (Dou et al. 2012), phenol mineralization (Suryaman et al. 2009), or *E. coli* inactivation (Pablos et al. 2012).

The aim of this research work is to compare not only the disinfection effectiveness of two types of TiO_2 , the standard TiO_2 Degussa P25 and a commercial suspension of nano- TiO_2 , but also the PPCP removal effectiveness of both catalysts. In a first approach, both types are characterized. Next, the effect of the feature of water is analyzed, assessing different TiO_2 doses and treatment times. In addition, postirradiation survival in the dark is studied after disinfection treatments. Finally, the separation through simple decantation and mechanical CFD and posterior reuse of the TiO_2 for disinfection and caffeine photo-degradation is evaluated.

Materials and methods

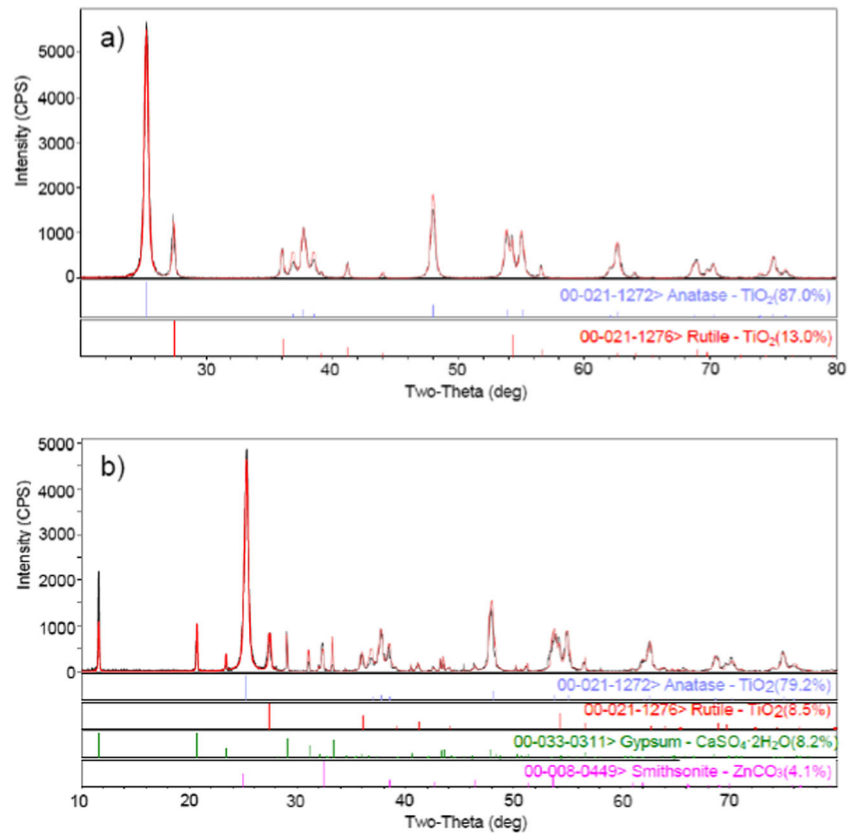
TiO_2 characterization

In this study, two types of commercial titanium dioxide were used: TiO_2 Degussa P25 (solid power), commercialized now by Evonik, and TiO_2 Levenger FN2 (aqueous suspension).

Crystalline phases were analyzed by X-ray diffraction (XRD) with a diffractometer Rigaku D/Max-2500, provided with a graphite monochromator to select the $Cu K\alpha$ radiation. Measure interval (2θ) went from 10 to 80° at a speed of 1.8°/min. Determination and quantification of phases and size particle calculus were carried out with the software MDI-Jade7 and the data base JCPDS-International Centre for Diffraction Data-2000. For the semiquantitative analysis of X-ray fluorescence (XRF), a sequential XRF spectrophotometer Thermo Electron ARL ADVANT'XP was used. This XRF equipment was provided with an X-ray tube with a frontal window of beryllium (Be) and a rhodium (Rh) anode, and it allows the semiquantitative detection of the elements between sodium (Na) and uranium (U). Particle morphology was studied by field emission scanning electron microscopy (FESEM) with a FESEM microscope Carl Zeiss MERLIN™ containing a secondary and retro-dispersed electrons detector.

Figure 1 presents the XRD patterns of both titanium dioxides catalysts. The peaks observed in the diffractogram of TiO_2 Degussa P25 (Fig. 1a) correspond to the crystalline phases of TiO_2 , anatase, and rutile, with a weight percentage of 87% and 13%, respectively. TiO_2 Levenger characterization (Fig. 1b) showed crystalline structures of gypsum $CaSO_4 \cdot H_2O$ (8%) and smithsonite $ZnCO_3$ (4%), along with the phases of TiO_2 , anatase

Fig. 1 XRD pattern of (a) TiO₂ Degussa P25 and (b) TiO₂ Levenger



(79%), and rutile (9%). Both types of titanium dioxide presented a similar ratio anatase/rutile. The results obtained by XRD were confirmed by the semiquantitative elemental analysis of X-ray fluorescence. Average particle size was calculated from the XRD data, resulting in 25 nm for TiO₂ Degussa P25 and 23 nm for TiO₂ Levenger. Figure 2 shows a FESEM image of both catalysts. While TiO₂ Degussa was formed just by homogeneous round particles, in TiO₂ Levenger the presence of bigger size (> 300 nm) particles with straight edges was also detected. Probably, these particles correspond to the CaSO₄·H₂O identified by XRD and XRF. TSS in TiO₂ Levenger was 106 g/l, which means a concentration of around 93 g/l TiO₂.

Bacterial inactivation experiments

Water samples

Bacterial inactivation assays were conducted in two types of water samples: sterile saline solution (NaCl solution) and simulated municipal wastewater treatment plant effluent (WWE). The sterile saline solution was prepared by addition of 0.9% (w/v) of NaCl (Panreac) to distilled water and subsequent sterilization. Afterward, the NaCl solution was inoculated with pure cells of *Escherichia coli* or *Enterococcus* sp. obtained from the culture in nutritive agar of wild strains isolated from

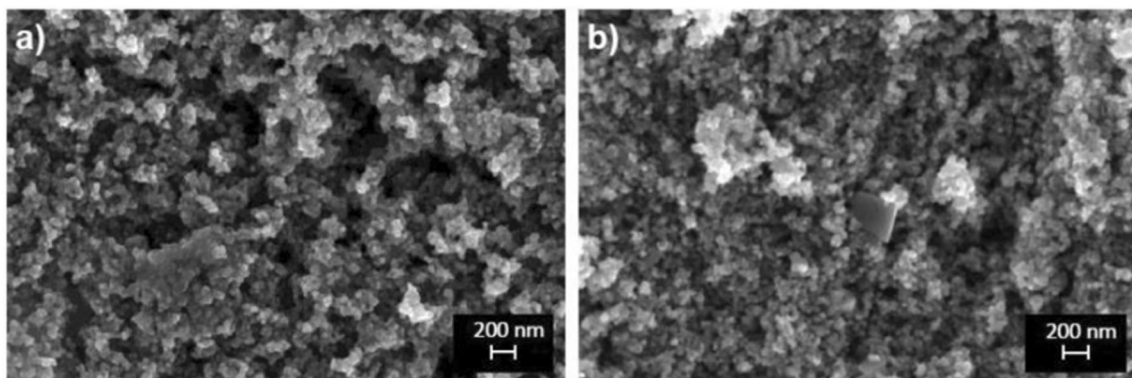


Fig. 2 FESEM images of (a) TiO₂ Degussa P25 and (b) TiO₂ Levenger

real wastewater treatment plant effluents (WWTPE), achieving an initial bacterial concentration of 10^{7-8} CFU/100 ml. The WWE was obtained from an activated sludge plant at laboratory scale described elsewhere (Mosteo et al. 2013, Rodríguez-Chueca et al. 2014a). This WWE sample naturally contains a consortium of bacteria typical from WWTPE, since it comes from an activated sludge reactor. Specifically, the bacteria *E. coli* and *Enterococcus* sp. are present in this sample in concentrations ranging between 10^5 and 10^6 CFU/100 ml. Table 1 summarizes the average values of the main physicochemical parameters of both water samples.

Microbiological analysis

When the microbiological concentration was high ($> 4 \cdot 10^3$ CFU/100 ml), the culture and enumeration of the bacteria were carried out according to the spread plate standard method 9215 C for both bacteria, making decimal dilutions when necessary. For lower concentrations ($< 4 \cdot 10^3$ CFU/100 ml), the analyses were conducted according to the membrane filtration methods UNE-EN ISO 9308-1 for *Escherichia coli* and UNE-EN ISO 7899-2 for *Enterococcus* sp. The samples were plated of MacConkey agar (Scharlau) for *E. coli*, and pink colonies were counted after 24-h incubation at 42 °C. For *Enterococcus* sp., the samples were plated on Slanetz and Bartley agar base (Scharlau), and dark red colonies were counted after 48-h incubation at 37 °C.

The enumeration of the bacteria was expressed as CFU (colony-forming units) per 100 ml of sample (CFU/100 ml). The bacterial inactivation was expressed as $\log(N_t/N_0)$, where N_0 was the initial bacterial concentration and N_t the remaining bacterial concentration at time t .

Experimental procedure

Control experiments Firstly, control experiments in both water matrices were performed in the dark to assess the effect of natural mortality, stirring, and presence of TiO_2 particles (1 g TiO_2 /l) on the inactivation of both bacteria. Bacterial concentration was measured in the reactors

containing 100 ml of sample at different times up to a maximum of 180 min.

Photo-inactivation experiments The photolytic and photocatalytic experiments were conducted in an Atlas Suntest CPS+/XLS+ solar chamber provided with a xenon lamp. This system enabled the reproduction of natural sunlight conditions in the laboratory. A quartz filter and an additional glass filter (Xenochrome 320) were used to cut off wavelengths below 320 nm, removing the UVB range. Therefore, the samples were exposed to wavelengths between 320 and 800 nm, mainly including the UVA and visible bands. All the essays were carried out with light intensity of 500 W/m^2 , which corresponds to the 50% of the light intensity of the midday equatorial solar radiation (Yuranova et al. 2004). The maximum temperature reached in the solar chamber was 35 °C, although the samples did not exceed 30 °C. Reactions were carried out with 100 ml of sample in sterile 250-ml quartz beakers with continuous stirring. Photolysis treatments were carried out with UVA-vis irradiation in the absence of TiO_2 . Photocatalytic treatments were conducted in the presence of UVA-vis irradiation and TiO_2 catalyst (TiO_2 Degussa P25 or TiO_2 Levenger). The effect of TiO_2 dose (0.25–2 g/l TiO_2) and time (0–180 min) was studied. Bacterial analyses were conducted immediately after the treatments. Moreover, the alkalinity and the pH of the samples were measured initially and after 60 min of irradiation in parallel experiments to avoid microbiological contamination of the samples. Alkalinity was determined by titration (Standard Method 2320 B), while pH was measured with a pH-meter CRISON GLP 21. All the experiments have been repeated at least twice, the represented values are the average, and standard deviation is not shown when its value is negligible.

Bacterial regrowth/survival experiments For regrowth or survival experiments, the samples (NaCl solution or WWE) were exposed for different times to UVA-vis irradiation in the absence or presence of 1 g/l TiO_2 (Degussa P25 or Levenger). Afterward, the samples were stored in the dark for 48 h, and bacterial concentration was periodically measured at 4 h, 24 h, and 48 h.

Table 1 Physicochemical characteristics of the water samples. Average values

Parameter	Sterile saline solution (NaCl solution)	Synthetic WWTP effluent (WWE)
pH	6.2	7.8
Conductivity ($\mu\text{S/cm}$)	13,200	777
Turbidity (NTU)	< 1	2
COD (mg O_2 /L)	< 2	22
DOC (mg C/L)	< 1	11
TSS (mg/L)	< 1	5
Alkalinity (mg CaCO_3 /L)	< 5	110
Hardness (mg CaCO_3 /L)	< 5	250

Caffeine photo-degradation

Water samples

Caffeine removal assays were conducted in two types of water samples: ultrapure water and WWTP. Ultrapure water was obtained by using an *Ecomatic* (WaserLab) ultrafiltration system. WWTP was collected from a 35,000 inhabitants wastewater plant located in the Ebro Basin in Spain.

Caffeine quantification

Caffeine (*Panreac, pharma grade*) quantification was carried via molecular absorption of the samples by means of a spectrophotometer *Helios UV-VIS ThermoSpectronic* (Delvadiya et al. 2011) at a wavelength of 272.5 nm. The experimental limit of detection (LOD) of this method was 0.3 mg/l, and its limit of quantification (LOQ) was 1.1 mg/l.

Experimental procedure

The photolytic and photocatalytic experiments were conducted in the same operational conditions as the inactivation tests, detailed in Sect. 2.2.3. The initial caffeine concentration was 45 mg/l, according to others research studies (Bernabeu et al. 2011, Prieto-Rodríguez et al. 2012, Rimoldi et al. 2017). Photocatalytic treatments were conducted in the presence of UVA-vis irradiation and TiO₂ catalyst (TiO₂ *Degussa P25* or TiO₂ *Levenger*). Reactions were carried out with 100 ml of sample in sterile 250-ml quartz beakers with continuous stirring. Photolysis treatments were conducted with UVA-vis irradiation in the absence of TiO₂. The effect of TiO₂ dose (0.25–2 g/l TiO₂) and time (0–180 min) was studied. All the experiments have been repeated at least twice, the represented values are the average, and standard deviation is not showed when its value is negligible.

TiO₂ separation and reuse

In order to study TiO₂ separation possibilities, decantation experiments were carried out in ultrapure water, NaCl solution, and WWE. The WWE matrix simulates the effluent of a real wastewater treatment plant. Samples containing 1-g TiO₂/l (TiO₂ *Degussa P25* or TiO₂ *Levenger*) were poured into 100-ml graduated cylinders, and TiO₂ was left settle. The evolution of the turbidity of the clarified upper phase was measured with a HANNA Instruments LP 2000 turbidimeter.

For each recovery experiment, four quartz reactors containing 100 ml of sample with 1-g TiO₂/L (TiO₂ *Degussa P25* or TiO₂ *Levenger*) were used. The samples fortified with caffeine and microorganisms were exposed to UVA-vis irradiation (320–800 nm, 500 W/m², 35 °C) with constant stirring. Next, microbiological and caffeine analyses of one of the

reactors were carried out. After that, the remaining samples were poured into 100-ml graduated cylinders for TiO₂ simple decantation. Once the phases were separated, the clarified treated water was carefully removed, and 100 ml of untreated sample were poured into each graduated cylinder, which already contained the used TiO₂. Simple decantation and mechanical CFD were also compared. The CFD involves two stirring steps: firstly, the coagulation was obtained by means of a *Jar-test SBS Floc tester* (200 rpm during 4 min) and, secondly, the flocculation (40 rpm during 15 min of stirring). These photocatalysis and mechanical CFD steps were repeated for four cycles.

Results and discussion

Bacterial inactivation

Control experiments

Figure 3 illustrates bacterial inactivation in the NaCl solution and in the WWE during the control assays. In general, stirring and presence of 1 g/l TiO₂ caused no decrease on bacterial concentration after 180 min in the dark.

Inactivation of *E. coli* was only produced in the saline solution with TiO₂ *Levenger* (Fig. 3a), achieving more than 1.5 log units inactivation within 180 min. Several authors have proved that the inactivation mechanism in photocatalysis implies the adsorption of the bacteria on the TiO₂ surface (Gogniat et al. 2006, Rizzo 2009, Pablos et al. 2013). Besides, in a NaCl-KCl solution, the Gram-negative bacterium *E. coli* adsorbed into TiO₂ might present alterations of its membrane integrity even in the absence of light (Gogniat et al. 2006). However, the Gram-positive bacterium *Enterococcus* sp. did not show inactivation in any of the control assays (Fig. 3b), meaning that there are some differences in the mode of action of TiO₂ depending on the type of cellular wall. Grieken et al. (van Grieken et al. 2010) observed a similar tendency of these bacteria in distilled water, showing the greater sensitivity of *E. coli* toward stress factors, such as stirring or presence of TiO₂ particles. In the WWE, almost no inactivation of any of the bacteria (< 0.3 log units) was observed in the controls after 180 min (Fig. 3c and d), which is in agreement with other studies (Rincón and Pulgarin 2004a, 2004b, van Grieken et al. 2010).

Photo-inactivation experiments

Figure 4 illustrates the photo-inactivation of *E. coli* and *Enterococcus* sp. in the saline solution and in the WWE, after 60 min of exposure to solar-simulated light (UVA-vis) in the absence or presence of different concentrations of TiO₂ ranging from 0.25 to 2.0 g/l. In general, no influence of the

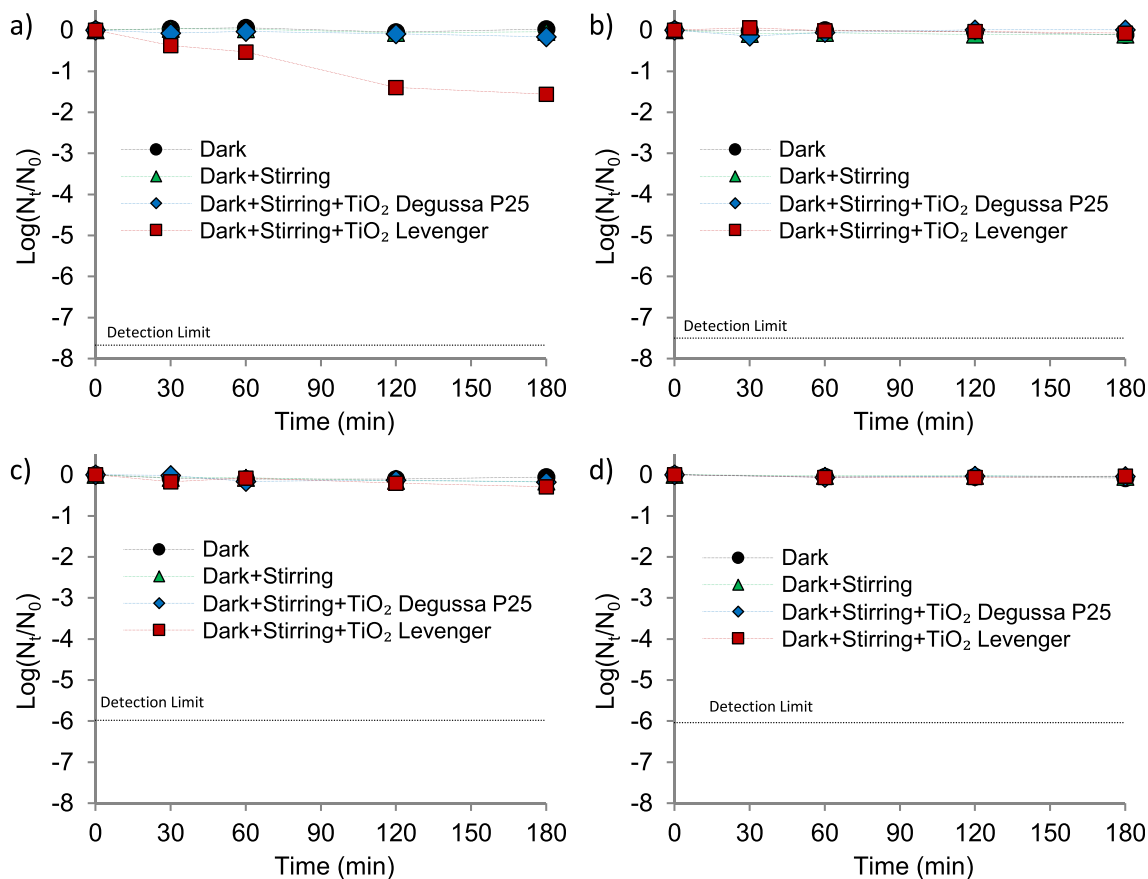


Fig. 3 Control experiments in the dark: **(a)** *Escherichia coli* inactivation in NaCl solution, **(b)** *Enterococcus* sp. inactivation in NaCl solution, **(c)** *Escherichia coli* inactivation in WWE, and **(d)** *Enterococcus* sp. inactivation in WWE

concentration or type of TiO₂ was observed, except for *Enterococcus* sp. in the saline solution (Fig. 4b). *E. coli* inactivation was fast in that matrix (Fig. 4a), reaching the detection limit within 60 min even with the lowest TiO₂ dose tested (0.25 g/l) and regardless of the type of TiO₂.

However, *Enterococcus* sp. disinfection in the saline solution presented several differences (Fig. 4b): the highest bacterial inactivation was obtained with TiO₂ Degussa P25, and in addition, increasing doses of *Levenger* TiO₂ produced higher removal of bacteria. Probably, similar trends might have been observed for *E. coli* inactivation if treatment time had been shorter. The lower efficiency of the TiO₂ *Levenger* might be attributed to the presence of inorganic compounds (CaSO₄·H₂O and ZnCO₃), which increased the pH (~7) and the alkalinity of the saline solution, whereas with TiO₂ *Degussa* P25, the pH slightly dropped (~5.5), and alkalinity was 0 mg/l CaCO₃ (Fig. 5). Despite the fact that variations of pH within that values might not have a huge impact on bacterial inactivation, the presence of even low concentrations of SO₄²⁻ and HCO₃⁻ can noticeably reduce the effectiveness of the process (Rincón and Pulgarin 2004a, 2004b). The ^{*}OH scavenge by HCO₃⁻ is well-known (Parsons 2004), and besides, increasing alkalinity produces agglomeration of TiO₂ particles, thus

decreasing availability of photo-generated holes for ROS production (Jefferson et al. 2016). Moreover, SO₄²⁻ can be easily adsorbed on TiO₂ surface, therefore inhibiting bacterial inactivation (Rincón and Pulgarin 2004a, 2004b). When the dose of *Levenger* TiO₂ was augmented, there was probably a competition between the larger availability of TiO₂ particles with its consequent production of ROS and the increasing inhibition effect of the anions.

In the WWE there was no effect of the type of TiO₂ on bacteria inactivation, and despite the slightly improvement with 1 g/l, the effect of the TiO₂ dose with the studied concentrations did not seem to be significant (Fig. 4c and d). Both TiO₂ have a similar ratio anatase/rutile, and so, it is reasonable that their photocatalytic activities are very alike.

Concerning the water matrix, it can be observed that disinfection efficiency was remarkably lower in the WWE (~1 log unit inactivation) (Fig. 4c and d) than in the saline solution (~7 log units inactivation) (Fig. 4a and b) for both TiO₂ and bacteria; consequently, it can be deduced that the water matrix has a huge influence on bacterial inactivation. Gogniat et al. (2006) point out that the adsorption of bacteria onto TiO₂ particles, which is a key step for disinfection by photocatalysis, is influenced by the water composition and

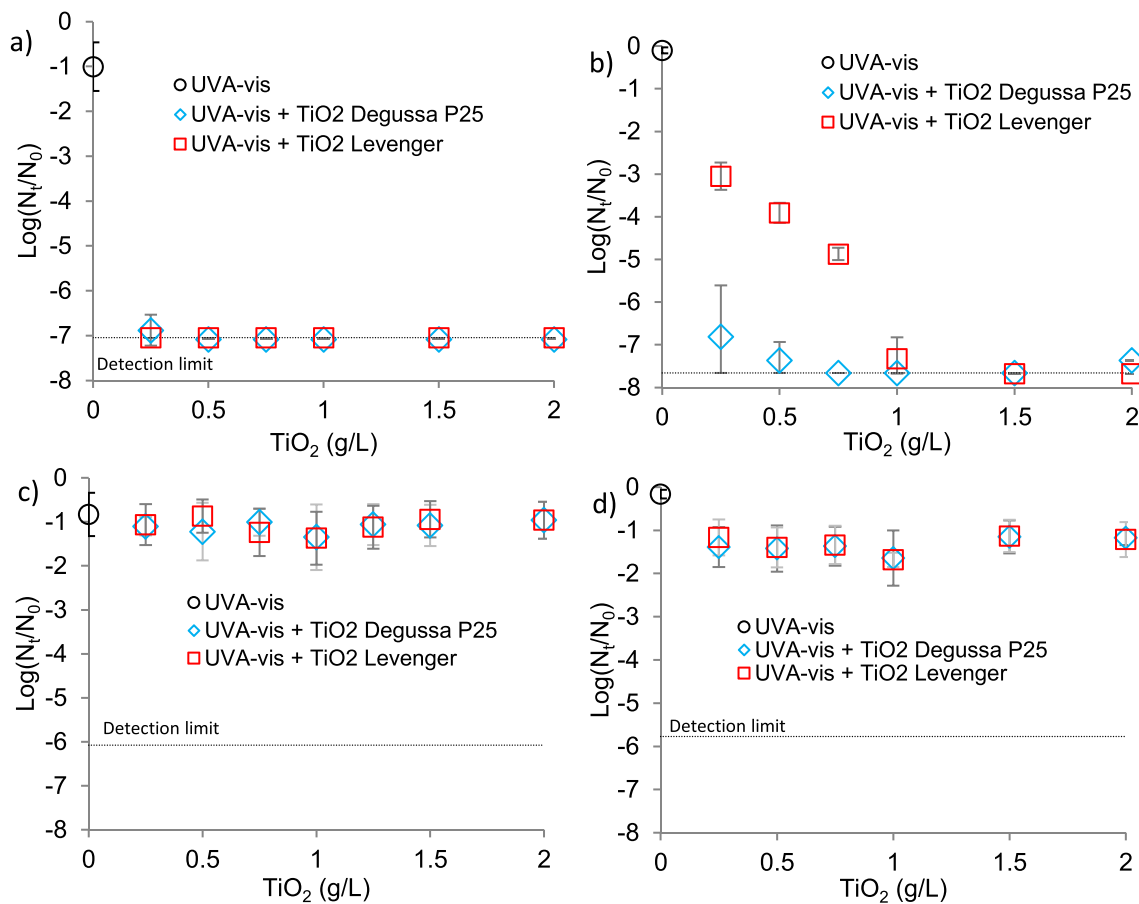


Fig. 4 Photocatalytic inactivation of *E. coli* and *Enterococcus* sp. in the presence of different TiO_2 concentrations after 60 min treatment: **(a)** *E. coli* inactivation in NaCl solution, **(b)** *Enterococcus* sp. inactivation

in NaCl solution, **(c)** *E. coli* inactivation in WWE, and **(d)** *Enterococcus* sp. inactivation in WWE

that in a NaCl-KCl solution this bound is very likely to happen. The WWE simulates the effluent of a real wastewater treatment plant, meaning that organic and inorganic substances, along with a consortium of microorganisms, were present in the sample. The higher the presence of these compounds, the lower the probability of interaction between the targeted bacteria and the photo-generated ROS is. Organic compounds compete with the bacteria for the adsorbing sites on the TiO_2 surface and can even block them (Drosos et al. 2015), thus enhancing the reaction of ROS with organic matter rather than with bacteria. Although some reactive intermediates (R^*) could be formed during the organic degradation (Rincón and Pulgarin 2004a, 2004b), their oxidative power would be lower than those of hydroxyl radical. Moreover, as previously mentioned, inorganic ions affect the sensibility of bacteria toward TiO_2 . Some of those anions, such as SO_4^{2-} and HCO_3^- , which are probably present in the WWE sample, can have a detrimental effect on the TiO_2 photocatalysis, while others might produce the inverse reaction. For instance, the Cl^- anion, which is in high concentration in the saline solution, might react with $^*\text{OH}$ -initiating chain reactions involving the formation of other free radicals such as HOCl^{*-} (Saran

et al. 1999, Diao et al. 2004). Finally, the presence of other microorganisms reduced the probability of light or $^*\text{OH}$ to reach the targeted bacteria.

Figure 6 represents the bacterial inactivation curves of *E. coli* and *Enterococcus* sp. during the photolytic (light alone) and photocatalytic (light + 1 g TiO_2/l) treatments in the saline solution and in the WWE. It can be observed that, in every case, disinfection increased with treatment time and that, in general, the UV-vis/ TiO_2 process produced faster and higher inactivation than light alone. During the photocatalytic treatment in the saline solution, total inactivation (-7 log units) was achieved within 15 min and 60 min, for *E. coli* and *Enterococcus* sp., respectively. However, in the WWE ~ 4.5 log units of *E. coli* and ~ 2.5 log units of *Enterococcus* sp. were removed when irradiating TiO_2 for 180 min. Figure 6a and b show some differences between the inactivation efficiency of the studied titanium dioxides. In the saline solution, TiO_2 Degussa P25 produced faster bacterial disinfection than Levenger TiO_2 . As previously discussed, the anions (SO_4^{2-} and HCO_3^-) introduced by the TiO_2 Levenger would have a detrimental effect on the catalyst efficiency, especially in the saline solution. On the contrary, both

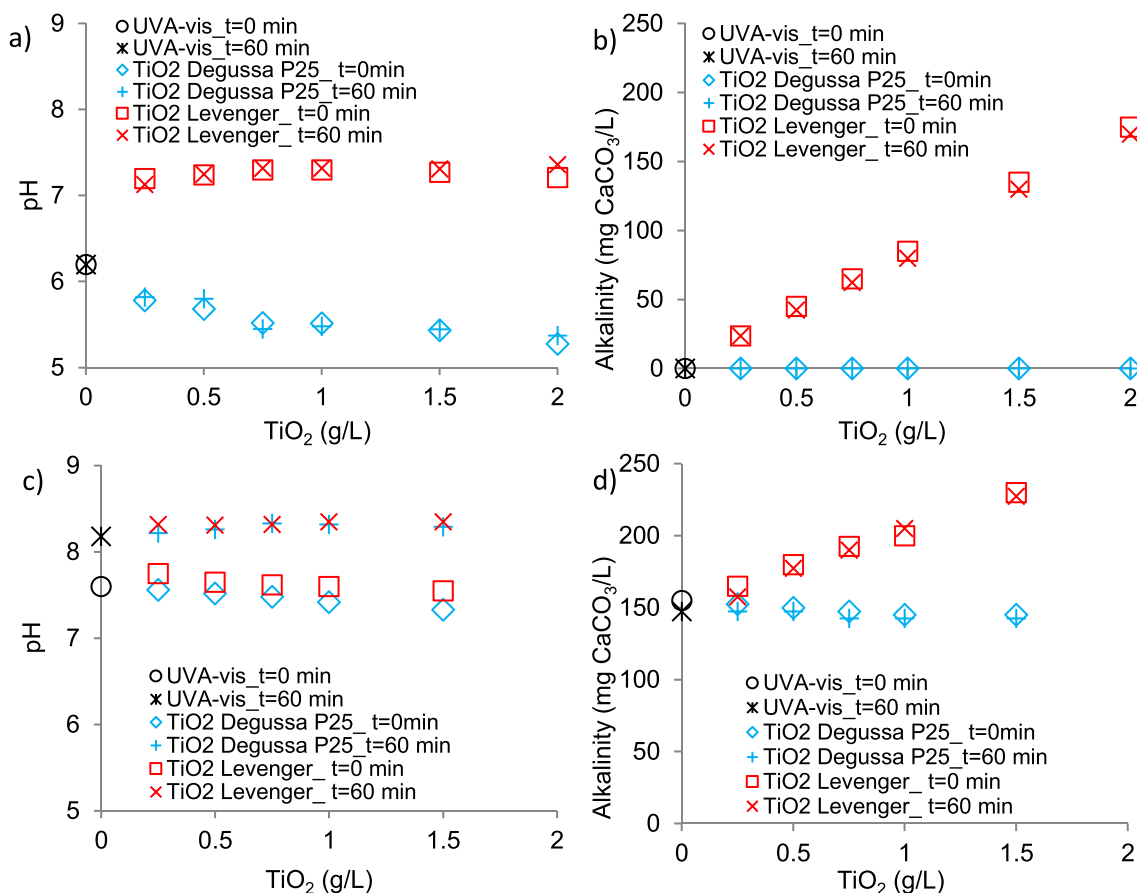


Fig. 5 pH and alkalinity values at time = 0 min and after 60 min irradiation in the presence of different TiO₂ concentrations: **(a)** pH in NaCl solution, **(b)** alkalinity in NaCl solution, **(c)** pH in WWE, and **(d)** alkalinity in WWE

catalysts exhibited the same inactivation in the WWE. Probably, in this matrix the addition of carbonates did not affect the process that much because there was already a high alkalinity (~150 mg/l CaCO₃).

It can be also noticed that the inactivation of each bacterium (*E. coli* or *Enterococcus* sp.) in the photolytic process followed a similar trend in the saline solution and in the WWE. On the contrary, in the photocatalytic process, disinfection efficiency differed greatly in each matrix. These results suggest that during the photolytic experiments, the mechanism of inactivation is mainly controlled by internal mechanisms inside the cell, such as intracellular (photo-)Fenton (Giannakis et al. 2016a, 2016b). However, the photocatalytic process is dominated by extracellular processes which produce lipid peroxidation of the cell membrane by ROS attack, initiating chain reactions and causing oxidative stress and DNA degradation, which eventually leads to cell death (Maness et al. 1999). Therefore, the environment surrounding the cell, i.e., the water matrix, has more influence on the inactivation efficiency in the photocatalytic treatments than in the photolytic ones.

Figure 6 shows a higher sensitivity of *E. coli* toward the treatments than *Enterococcus* sp. The different composition of

their cellular wall (Willey et al. 2009) might cause this difference of behavior. Gram-negative bacteria, such as *E. coli*, have an outer membrane which is composed of lipids and polysaccharides susceptible of being oxidized by ROS. Nevertheless, the outer part of an *Enterococcus* sp. membrane consists of a thick layer of peptidoglycan, a peptide-cross-linked polysaccharide matrix, which might impart higher resistance to the cell (Dalrymple et al. 2010).

Bacterial regrowth/survival experiments

Figure 7 illustrates the bacterial regrowth or survival in the dark after the photo-treatments. Figure 7a shows the *E. coli* postirradiation events in saline solution. No regrowth of *E. coli* was observed in this matrix after applying the photocatalytic treatment even during a short period of 15 min. Nevertheless, *E. coli* behavior after the photolytic treatment differed depending on the irradiation exposure time. For short periods of treatment (i.e., 15 min), a small regrowth could be observed within 48 h, while for longer exposure (i.e., 60 min), the *E. coli* population slightly diminished. *Enterococcus* sp. survival in NaCl is shown in Fig. 7b. This Gram-positive bacterium was completely removed in the presence of 1 g/l

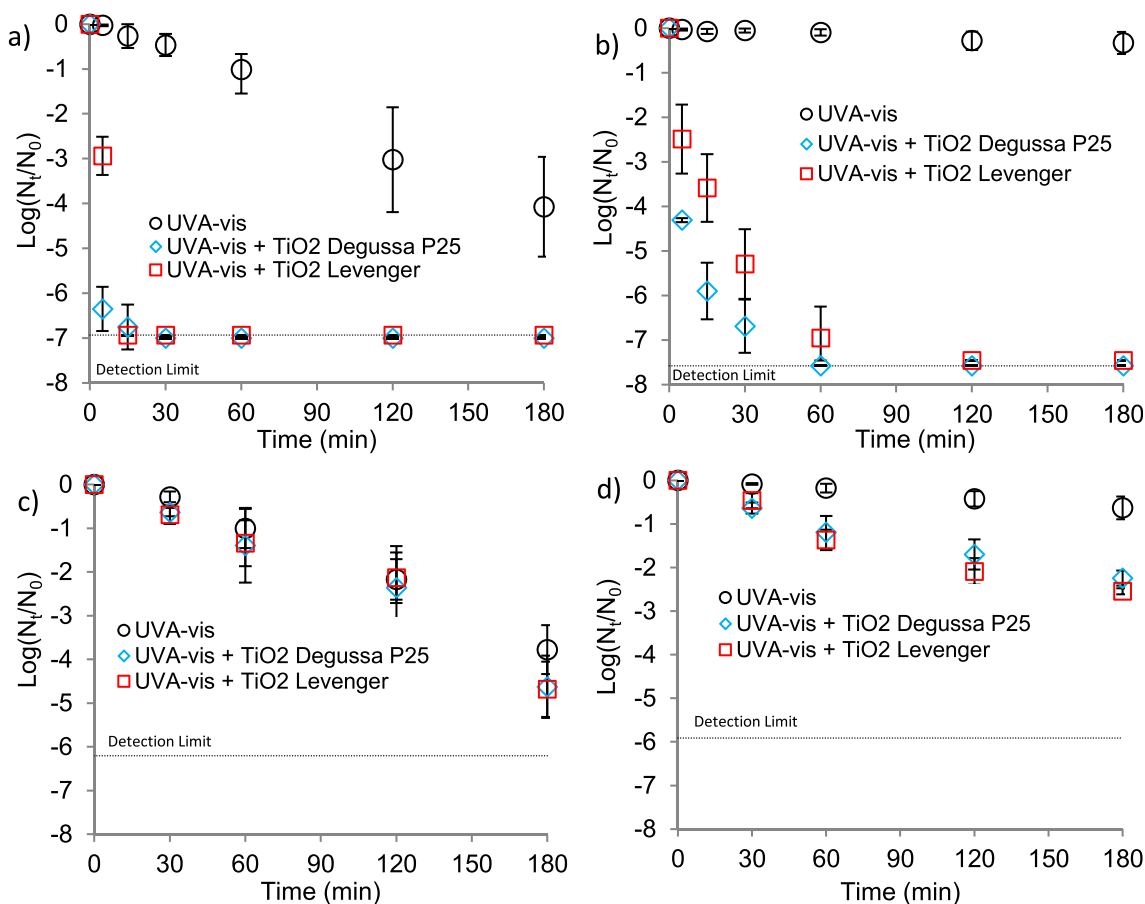


Fig. 6 Bacterial inactivation in the absence and presence of 1 g/l TiO₂ Degussa P25 or TiO₂ Levenger (a) *E. coli* inactivation in NaCl solution, (b) *Enterococcus* sp. inactivation in NaCl solution, (c) *E. coli* inactivation in WWE, and (d) *Enterococcus* sp. inactivation in WWE

TiO₂ within 60 min, and it survived no longer than 4 h when treated for 15 min with TiO₂ Degussa or Levenger. Unlike *E. coli*, *Enterococcus* sp. population stayed nearly constant for 48 h in the dark even when previously photo-treated for 60 min with UVA-vis light.

In the WWE, the concentration of *E. coli* submitted to TiO₂ photocatalysis decreased after 4 h of dark storage (Fig. 7c). Then, slow regrowth took place within the next 48 h for bacteria previously treated for 30 min, while for 60-min photo-treated cells a small reduction of the concentration was observed. A similar tendency of *E. coli* survival was observed in the absence of TiO₂ in this matrix. *Enterococcus* sp. concentration in WWE (Fig. 7d) remained almost invariable within 48 h when photo-treated, by photolysis or photocatalysis, for 30 min. Several conclusions can be extracted from Fig. 7. For instance, both types of TiO₂ led to similar survival opportunities; consequently, cellular damage caused by them must have been the same. Moreover, except for *E. coli* in WWE, the disinfection power of TiO₂ was higher than that of light alone, reducing the potential risk of regrowth. This risk also diminished as treatment time increased, because the longer the exposure to photolysis or photocatalysis, the higher the light dose received will be (Giannakis et al. 2015), and therefore, the oxidation of organic

matter constituting the microorganisms will increase (Dalrymple et al. 2010). The matrix composition had an enormous influence as well, not only on bacterial disinfection efficiency but also on bacterial survival afterward, favoring it in the WWE sample rather than in the saline solution. Despite several DNA repair mechanisms (Sinha and Hader 2002) and protective mechanisms against oxidative stress, such as enzymatic defense (Hoerter et al. 2005), can take place, exposure to TiO₂ in NaCl caused intensive ROS attack which led to damaged cells unable to heal the injuries. However, in the WWE bacteria concentration experienced little variation after the TiO₂ treatment. This matrix was more complex and contained organic matter which might have reacted with the photo-generated ROS, thus reducing the probability of ^{*}OH-bacteria interaction. In addition, availability of nutrients in the WWE benefits bacterial survival, while salinity of the NaCl solution can have a detrimental effect on photo-treated cells recovery (Giannakis et al. 2014). Previous studies have also proved that the increase of the matrix complexity (e.g., distilled water vs. simulated treated wastewater) leads to the reduction in efficiency of the applied OAP on bacterial inactivation (Rodríguez-Chueca et al. 2012; Rodríguez-Chueca et al. 2014b). Finally, *E. coli* presented more sensitivity than *Enterococcus* sp. to the treatments, but

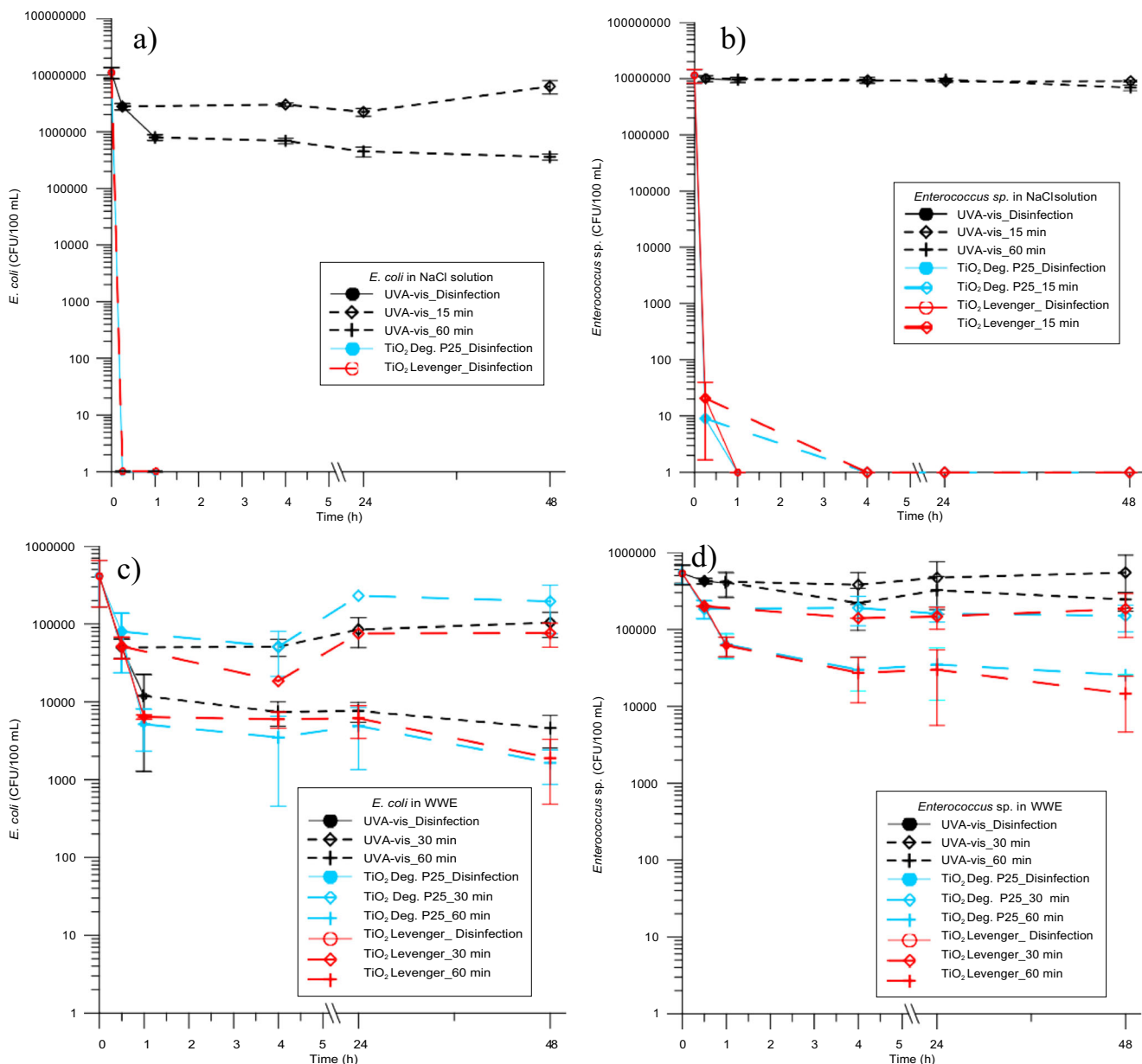


Fig. 7 Bacterial regrowth after photolytic and photocatalytic treatments with 1 g/l TiO₂ in **(a)** *E. coli* in NaCl solution, **(b)** *Enterococcus* sp. in NaCl solution, **(c)** *E. coli* in WWE, and **(d)** *Enterococcus* sp. in WWE

survival patterns were similar for both bacteria, showing little regrowth after short exposures and slight decay in population when photo-treated longer.

Caffeine degradation

Photo-degradation experiments

After verifying that there is not any observable effect of photolysis, photo-degradation experiments were conducted. Figure 8 illustrates the photo-degradation of caffeine in the ultrapure water solution and in the WWTP, after 120 min of exposure to solar-simulated light (UVA-vis) in the absence

or present of different concentration of TiO₂ ranging from 0.5 to 2 g/l. The results show little influence of the type of TiO₂: caffeine photo-degradation results are similar of both catalysts. Similar results were obtained in terms of caffeine photo-degradation (Vaiano et al. 2018), using TiO₂ nanotubes (Athanasakou et al. 2018), and slightly inferior of the photo-degradation obtained using of ZnO-ZnAl₂O₄ as catalyst (Elhalil et al. 2017).

Furthermore, this photo-degradation difference between both catalysts tends to decrease when the catalyst dose increases. The TiO₂ *Levensger* lower efficiency might be attributed to the presence of inorganic compounds (CaSO₄·H₂O and ZnCO₃), which tend to increase the pH and alkalinity.

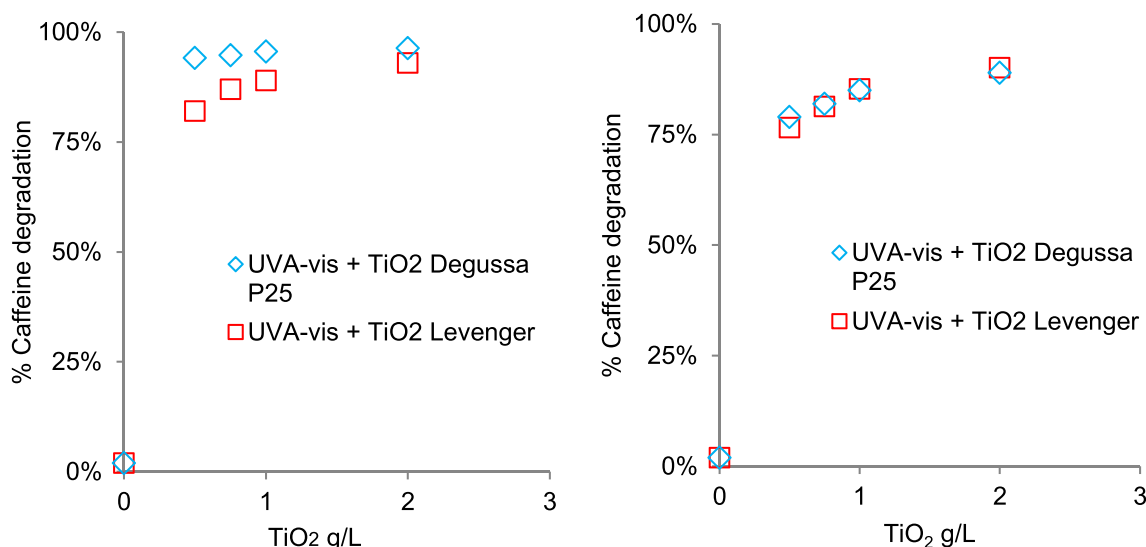


Fig. 8 Photocatalytic degradation of caffeine in the presence of different TiO₂ Degussa P25 or TiO₂ Levenger concentrations (120 min irradiation): (a) ultrapure water solution and (b) WWTPPE

Regardless the type of catalyst, Fig. 8a and b show that the matrix affects to the catalytic photo-degradation process, the same trend is observed in both types of catalyst: the percentage of caffeine degradation is higher in ultrapure water than in WWTPPE, as occurred in terms of photo-disinfection. This might be associated to the different initial pH of the two matrix (pH_{ultrapure water} = 5.64, pH_{WWTPPE} = 7.43) and to the presence of organic matter in the latter too. It has been also demonstrated that the maximum photocatalytic activity is obtained at pH = 5 for *Degussa* P25 (Arfanis et al. 2017).

TiO₂ separation and reuse

TiO₂ separation

This experiment intends to perform a simple technique for water clarification and TiO₂ recovery that might allow its posterior reuse. Evolution of turbidity was measured as a representative parameter of the TiO₂ separation. Figure 9 shows minor differences between the two catalysts. Simple decantation of TiO₂ *Levenger* was slightly faster than TiO₂ *Degussa* P25 in the saline solution, while the opposite tendency occurred in the WWE. Nanoparticles aggregation is more favorable as the zeta potential approaches the point of zero charge, which is related to the pH of the solution (Hsiung et al. 2016). Considering the pH of each sample (Fig. 5a and c), the pH of zero point charge for the studied catalysts must be around pH 7; therefore, the closer the pH is to this value, the faster the decantation will be. Applying a previous mechanical CFD, both catalysts show similar results, and TiO₂ *Levenger* decantation after the mechanical treatment was again slightly faster than TiO₂ *Degussa* P25 in the saline solution and in the WWE.

Figure 9 also shows two different stages in every case: fast decantation and slow decantation. For the simple decantation treatment, TiO₂ decantation was faster during 60 min: the turbidity decreases 95% in the two water samples, and a high fraction of the turbidity was reduced. After that initial period, the remaining TiO₂ particles settled rather slowly reaching a turbidity decrease of 97.5% after 24 h of decantation. Similar results were obtained by induced accelerated sedimentation of TiO₂, so it proposed a microfiltration process as final TiO₂ separation stage.

By comparison, after applying the mechanical coagulation (4 min) and flocculation (15 min), the first stage (faster decantation) achieves a turbidity decrease of more than 95% in only 10 min in contrast with the 60 min required in the simple decantation, while the second stage (slow decantation) reaches the practically total recovery in 2 h (99.7% of catalyst recovery) instead of the 24 h required in the simple decantation.

TiO₂ reuse for bacterial inactivation

Figure 10 illustrates bacterial inactivation per gram of TiO₂ (Log(N_t/N₀)/g TiO₂) during four cycles of TiO₂ reuse. In NaCl (Fig. 9a), maximum efficiency (~7 log units removal/g TiO₂) was achieved with both catalysts during the four cycles. Besides, bacterial adsorption on the reused TiO₂ and its potential contamination were discarded by placing ~0.5 g of used TiO₂ in 100-ml peptone water at room temperature in the dark and checking bacterial absence after 24 h.

In WWE (Fig. 10b), inactivation remained almost invariable for the four cycles, although in some cases, there was a small loss of TiO₂ efficiency. When organic matter is present in the water, it can be adsorbed onto the TiO₂ surface, especially small- and medium-size fractions (Drosos et al. 2015).

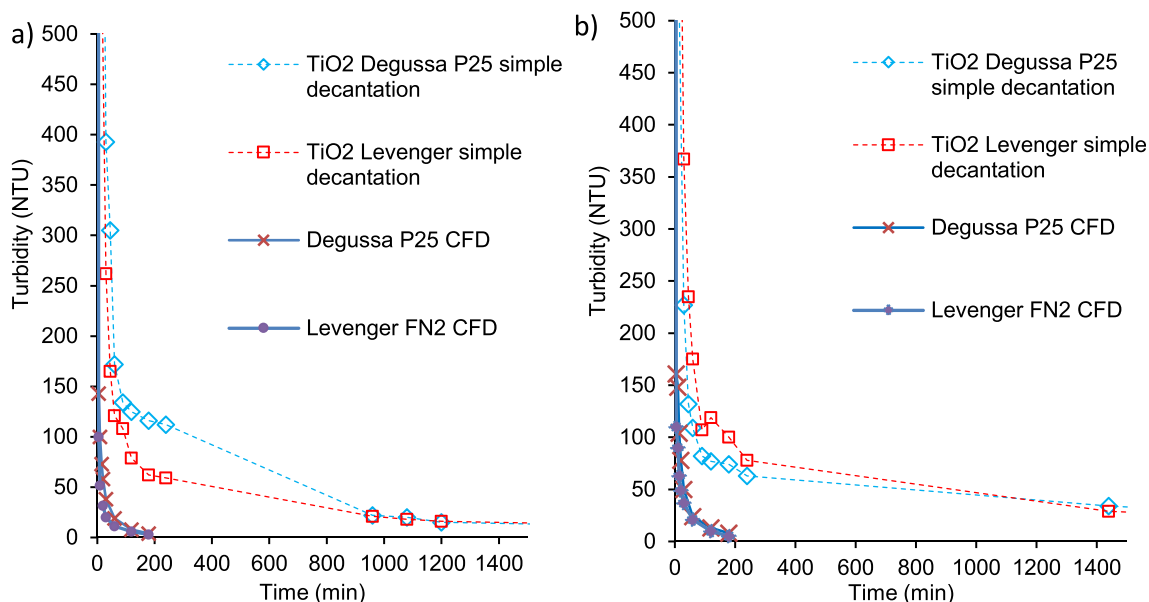


Fig. 9 Turbidity evolution during the decantation experiments with 1 g/l TiO₂ in (a) NaCl solution and (b) WWE

Despite the fact that part of the organic matter can be degraded by the photo-generated ROS (Wiszniewski et al. 2004, Yang and Lee 2006), some of it might accumulate during the cycles, thus reducing the probability of electrons, hole sites, and ROS to react with bacteria.

TiO₂ reuse for caffeine photo-degradation

Figure 11 illustrates caffeine of catalytic photo-degradation after 120 min of reaction using each catalyst in a concentration of 1-g TiO₂/l in ultrapure water. The results show that there are significant differences between the catalysts. TiO₂ Degussa P25 presents a loss of efficiency: in the second cycle photo-degradation of caffeine decreases 24.6% and after four cycles 28.5% in regard to the photo-degradation resulting of the first use. Meanwhile TiO₂ Levenger keeps its efficiency practically constant during four cycles, showing a decrease of 2.3% in the fourth use regarding the first cycle.

The results are similar for WTTPE, and TiO₂ Degussa P25 shows a loss of efficiency of 9% after the first cycle, what means less than a half of reduction conducted in ultrapure water. This can be attributed to the fact that the initial caffeine degradation is lower due to the presence of scavengers such as organic matter and the different pH and alkalinity of the water matrix. However, TiO₂ Levenger keeps its caffeine photo-degradation efficiency almost constant after four cycles. The same trend was reported in terms of TiO₂ reusability for degradation of fluoroquinolones.

Conclusions

Photocatalysis led to greater disinfection and caffeine degradation efficiency than light alone, since ROS formation is favored in the presence of TiO₂. Inactivation and photo-degradation results were similar for both TiO₂ types; therefore, their photocatalytic activity is very alike, which is in

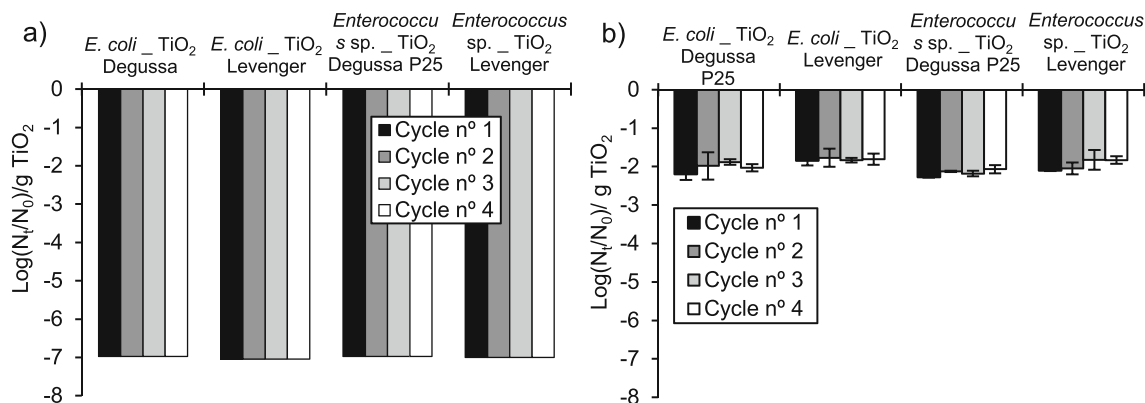


Fig. 10 Bacterial inactivation after several cycles of TiO₂ reuse: (a) NaCl solution (30 min irradiation) and (b) WWE (60-min irradiation)

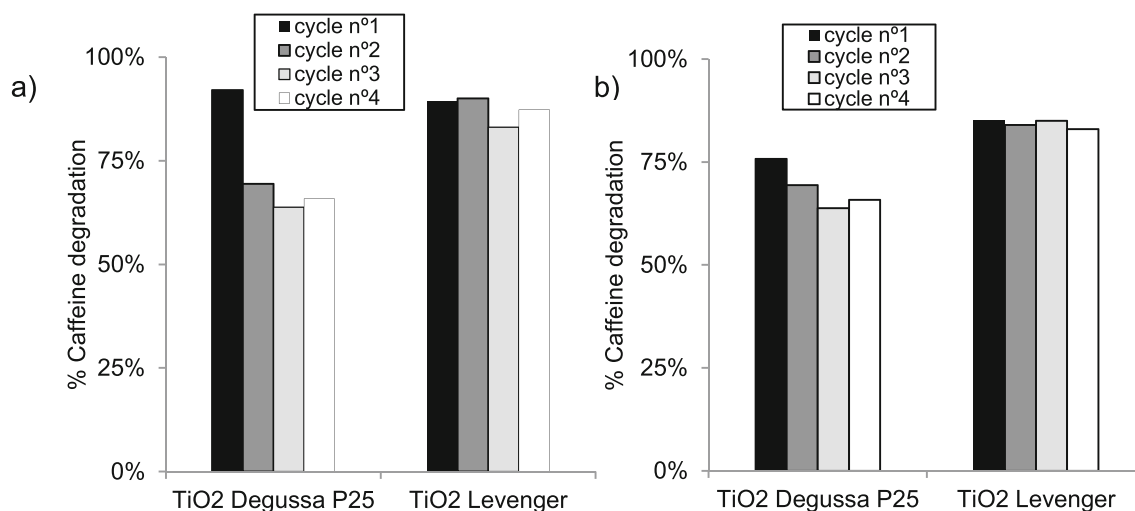


Fig. 11 Caffeine photocatalytic degradation after several cycles of TiO₂ reuse (120-min irradiation, 1-g TiO₂/l): **(a)** Ultrapure water solution and **(b)** WWTPE

accordance with their comparable ratios anatase/rutile. Small differences found in the behavior of these catalysts might be attributed to the presence of inorganic compounds in TiO₂ *Levensger*, which increase alkalinity and sulfate content and might reduce ROS-bacteria interaction, especially in matrices with low alkalinity, such as the saline solution. Doses ranging from 0.25 to 2 g/l TiO₂ produced similar reduction of bacteria population in the WWE.

Water composition had a significant effect on the photocatalytic process. The photo-degradation of caffeine and photo-disinfection reached in the ultrapure or saline solution are always superior to the photo-degradation and photo-disinfection conducted in WWTPE. However, when applying UVA-vis irradiation, the inactivation tendency was the same in both water matrices, reflecting the fact that, in photolysis, cell attack is mainly caused by an internal process, whereas in photocatalysis, bacterial inactivation starts with external ROS attack.

The efficiency of the processes differed depending on the type of the targeted bacteria as well, being *E. coli* (Gram-negative) more sensitive toward the treatments than *Enterococcus* sp. (Gram-positive), especially when applying photolysis. The thick layer of peptidoglycan confers resistance to *Enterococcus* sp. cells, while the membrane of *E. coli* is more likely to be oxidized by ROS. Nevertheless, both bacteria showed similar survival trends after the photo-treatments. In order to ensure that no regrowth takes place, cell exposure has to be long enough to cause irreparable damage. Concerning the catalyst separation, TiO₂ simple decantation allowed the recovery of 95% of the catalyst in 1 hour, whereas for the 97.5% of recovery, 1 day was required. In contrast, the applied mechanical CFD allows the recovery of 95% of both catalyst in 10 min and 99.7% in 2 hours.

Finally, reuse of the recovered TiO₂ for bacterial inactivation was successfully implemented during four cycles, with

negligible loss of the catalyst efficiency in NaCl and slight reduction of photo-activity in WWE. Nevertheless, respect to the caffeine photo-degradation, TiO₂ *Degussa P25* losses 28.5% of its efficiency after four cycles in ultrapure water solution, while TiO₂ *Levensger* only loses 2.3% in regard to the efficiency of the first cycle; the same trend was observed in WTTPE.

Funding information This work was financed by DGA-FSE Research Team “Water and Environmental Health” (T51_17R) and by the Project “Research study for the improvement of the quality of effluents from urban wastewater treatment plants and landfills, located in the Foral Community of Navarra (Spain)”, funded by NILSA.

References

Adegoke Anthony A, Faleye Adekunle C, Stenström Thor A (2018) Residual antibiotics, antibiotic resistant superbugs and antibiotic resistance genes in surface water catchments: public health impact. *Phys Chem Earth A/B/C* 105:177–183

Arfanis MK, A. P, Moustakas NG, Triantis TM, Kontos AG, Falaras P (2017) Photocatalytic degradation of salicylic acid and caffeine emerging contaminants using titania nanotubes. *Chem Eng J* 310: 525–536

Athanasekou CP, Likodimos V, Falaras P (2018) Recent developments of TiO₂ photocatalysis involving advanced oxidation and reduction reactions in water. *J Environ Chem Eng* 6:7386–7394

Augugliaro V, Litter M, Palmisano L, Soria J (2006) The combination of heterogeneous photocatalysis with chemical and physical operations: a tool for improving the photoprocess performance. *J Photochem Photobiol C: Photochem Rev* 7(4):127–144

Bernabeu, A., Vercher, R.F., Santos-Juanes, L., Simón, P.J., Lardín, C., Martínez, M.A., and J. A. Vicente, González, R., Llosá, C., Arques, A., Amat, A.M., 2011. (2011). "Solar photocatalysis as a tertiary treatment to remove emerging pollutants from wastewater treatment plant effluents." *Catal Today* 161: 235–240

Dalrymple OK, Stefanakos E, Trotz MA, Goswami DY (2010) A review of the mechanisms and modeling of photocatalytic disinfection. *Appl Catal B Environ* 98(1–2):27–38

- Delvadiya K, Kimbahune R, Kabra P, Patel P (2011) Spectrophotometric simultaneous analysis of paracetamol, propyphenazone and caffeine in tablet dosage forms. *J Pharm Pharm Sci* 3:170–174
- Diao HF, Li XY, Gu JD, Shi HC, Xie ZM (2004) Electron microscopic investigation of the bactericidal action of electrochemical disinfection in comparison with chlorination, ozonation and Fenton reaction. *Process Biochem* 39(11):1421–1426
- Dou L, Gao L, Yang X, Song X (2012) Hierarchical architectures TiO₂: pollen-induced synthesis, remarkable crystalline-phase stability, tunable size, and reused photo-catalysis. *J Hazard Mater* 203–204: 363–369
- Drosos M, Ren M, Frimmel FH (2015) The effect of NOM to TiO₂: interactions and photocatalytic behavior. *Appl Catal B Environ* 165:328–334
- Elhalil AE, Machrouhi R, Sadiq A, Abdennouri M, Qourzal M, Barka S, N. (2017) Photocatalytic degradation of caffeine by ZnO-ZnAl₂O₄ nanoparticles derived from LDH structure. *J Environ Chem Eng* 5:3719–3726
- Feitz AJ, Boyden BH, Waite TD (2000) Evaluation of two solar pilot scale fixed-bed photocatalytic reactors. *Water Res* 34(16):3927–3932
- Giannakis S, Merino Gamo AI, Darakas E, Escalas-Cañellas A, Pulgarin C (2014) Monitoring the post-irradiation *E. coli* survival patterns in environmental water matrices: implications in handling solar disinfected wastewater. *Chem Eng J* 253:366–376
- Giannakis S, Darakas E, Escalas-Cañellas A, Pulgarin C (2015) Solar disinfection modeling and post-irradiation response of *Escherichia coli* in wastewater. *Chem Eng J* 281:588–598
- Giannakis S, López MIP, Spuhler D, Pérez JAS, Ibáñez PF, Pulgarin C (2016a) Solar disinfection is an augmentable, in situ-generated photo-Fenton reaction—part 2: a review of the applications for drinking water and wastewater disinfection. *Appl Catal B Environ* 198:431–446
- Giannakis S, Polo López MI, Spuhler D, Sánchez Pérez JA, Fernández Ibáñez P, Pulgarin C (2016b) Solar disinfection is an augmentable, in situ-generated photo-Fenton reaction—part 1: a review of the mechanisms and the fundamental aspects of the process. *Appl Catal B Environ* 199:199–223
- Gogniat G, Thyssen M, Denis M, Pulgarin C, Dukan S (2006) The bactericidal effect of TiO₂ photocatalysis involves adsorption onto catalyst and the loss of membrane integrity. *FEMS Microbiol Lett* 258(1):18–24
- Gumy D, Rincon AG, Hajdu R, Pulgarin C (2006) Solar photocatalysis for detoxification and disinfection of water: different types of suspended and fixed TiO₂ catalysts study. *Sol Energy* 80(10): 1376–1381
- Heckman MA, W. J, De Mejia EG (2010) Caffeine (1, 3, 7-trimethylxanthine) in foods: a comprehensive review on consumption, functionality, safety, and regulatory matters. *Food Sci* 75(3): R77–R87
- Hoerter JD, Arnold AA, Kuczynska DA, Shibuya A, Ward CS, Sauer MG, Gizachew A, Hotchkiss TM, Fleming TJ, Johnson S (2005) Effects of sublethal UVA irradiation on activity levels of oxidative defense enzymes and protein oxidation in *Escherichia coli*. *J Photochem Photobiol B Biol* 81(3):171–180
- Hsiung C-E, Lien H-L, Galliano AE, Yeh C-S, Shih Y-h (2016) Effects of water chemistry on the destabilization and sedimentation of commercial TiO₂ nanoparticles: role of double-layer compression and charge neutralization. *Chemosphere* 151:145–151
- Jefferson B, Jarvis P, Bhagianathan GK, Smith H, Autin O, Goslan EH, MacAdam J, Carra I (2016) Effect of elevated UV dose and alkalinity on metaldehyde removal and THM formation with UV/TiO₂ and UV/H₂O₂. *Chem Eng J* 288:359–367
- Keller AA, Wang H, Zhou D, Lenihan HS, Cherr G, Cardinale BJ, Miller R, Ji Z (2010) Stability and aggregation of metal oxide nanoparticles in natural aqueous matrices. *Environ Sci Technol* 44(6):1962–1967
- Kidd KA, B. PJ, Mills KH, Palace VP, Evans RE, Lazorchak JM, Flick RW (2007) Disrupting queer inclusion. *Proc Natl Acad Sci U S A* 104:8897–8901
- Malato S, Fernández-Ibáñez P, Maldonado MI, Blanco J, Gernjak W (2009) Decontamination and disinfection of water by solar photocatalysis: recent overview and trends. *Catal Today* 147(1):1–59
- Maness PC, Smolinski S, Blake DM, Huang Z, Wolfrum EJ, Jacoby WA (1999) Bactericidal activity of photocatalytic TiO₂ reaction: toward an understanding of its killing mechanism. *Appl Environ Microbiol* 65(9):4094–4098
- Mosteo R, Ormad MP, Goni P, Rodríguez-Chueca J, García A, Clavel A (2013) Identification of pathogen bacteria and protozoa in treated urban wastewaters discharged in the Ebro River (Spain): water reuse possibilities. *Water Sci Technol* 68(3):575–583
- Ollis DF (2003) Integrating photocatalysis and membrane technologies for water treatment. *Ann N Y Acad Sci* 984:65–84
- Pablos C, Van Grieken R, Marugañ J, Muñoz A (2012) Simultaneous photocatalytic oxidation of pharmaceuticals and inactivation of *Escherichia coli* in wastewater treatment plant effluents with suspended and immobilised TiO₂. *Water Sci Technol* 65(11): 2016–2023
- Pablos C, van Grieken R, Marugañ J, Chowdhury I, Walker SL (2013) Study of bacterial adhesion onto immobilized TiO₂: effect on the photocatalytic activity for disinfection applications. *Catal Today* 209:140–146
- Parsons S (2004) Advanced oxidation processes for water and wastewater treatment. IWA
- Prieto-Rodríguez L, Miralles-Cuevas S, Oller I, Agüera A, Puma GL, Malato S (2012) Treatment of emerging contaminants in wastewater treatment plants (WWTP) effluents by solar photocatalysis using low TiO₂ concentrations. *J Hazard Mater* 211–212:131–137
- Rimoldi L, Meroni D, Falletta E, Pifferi V, Falciola L, Cappelletti G, Ardizzone S (2017) Emerging pollutant mixture mineralization by TiO₂ photocatalysts. The role of the water medium. *Photochem Photobiol Sci* 16:60–66
- Rincón A-G, Pulgarin C (2004a) Bactericidal action of illuminated TiO₂ on pure *Escherichia coli* and natural bacterial consortia: post-irradiation events in the dark and assessment of the effective disinfection time. *Appl Catal B Environ* 49(2):99–112
- Rincón A-G, Pulgarin C (2004b) Effect of pH, inorganic ions, organic matter and H₂O₂ on *E. coli* K12 photocatalytic inactivation by TiO₂: implications in solar water disinfection. *Appl Catal B Environ* 51(4):283–302
- Rizzo L (2009) Inactivation and injury of total coliform bacteria after primary disinfection of drinking water by TiO₂ photocatalysis. *J Hazard Mater* 165(1–3):48–51
- Rodríguez-Chueca J, Mosteo R, Ormad MP, Ovelleiro JL (2012) Factorial experimental design applied to *Escherichia coli* disinfection by Fenton and photo-Fenton processes. *Sol Energy* 86(11): 3260–3267
- Rodríguez-Chueca J, Mediano A, Ormad MP, Mosteo R, Ovelleiro JL (2014a) Disinfection of wastewater effluents with the Fenton-like process induced by electromagnetic fields. *Water Res* 60:250–258
- Rodríguez-Chueca J, Polo-López MI, Mosteo R, Ormad MP, Fernández-Ibáñez P (2014b) Disinfection of real and simulated urban wastewater effluents using a mild solar photo-Fenton. *Appl Catal B Environ* 150–151:619–629
- Rodríguez-Gil JLC, Dafouz N, Valcárcel R (2018) Caffeine and paraxanthine in aquatic systems: global exposure distributions and probabilistic risk assessment J.L. *Sci Total Environ* 612:1058–1071
- Saran M, Beck-Speier I, Fellerhoff B, Bauer G (1999) Phagocytic killing of microorganisms by radical processes: consequences of the reaction of hydroxyl radicals with chloride yielding chlorine atoms. *Free Radic Biol Med* 26(3–4):482–490

- Sinha RP, Hader DP (2002) UV-induced DNA damage and repair: a review. *Photochem Photobiol Sci* 1(4):225–236
- Suryaman D, Hasegawa K, Kagaya S, Yoshimura T (2009) Continuous mineralization of concentrated phenol dissolved in an electrolyte-containing tap water by integrating biological-photocatalytic treatment with TiO₂ separation: utilization of sunlight and reuse of TiO₂. *Environ Technol* 30(3):215–224
- Vaiano VM, Sacco M, Olga (2018) UV-LEDs floating-bed photoreactor for the removal of caffeine and paracetamol using ZnO supported on polystyrene pellets. *Chem Eng J* 350:703–713
- Van Gerven T, Mul G, Moulijn J, Stankiewicz A (2007) A review of intensification of photocatalytic processes. *Chem Eng Process Process Intensif* 49(9 SPEC. ISS):781–789
- van Grieken R, Marugán J, Pablos C, Furones L, López A (2010) Comparison between the photocatalytic inactivation of Gram-positive *E. faecalis* and Gram-negative *E. coli* faecal contamination indicator microorganisms. *Appl Catal B Environ* 100(1–2):212–220
- Vitor JP, Vilar RAT-P (2018) Advanced oxidation technologies: state-of-the-art in Ibero-American countries. *Environ Sci Pollut Res* 26(5):4153–4154
- WHO (2006) Guidelines for the safe use of wastewater, excreta and greywater. WHO
- WHO (2016) Protecting surface water for health: identifying, assessing and managing drinking-water quality risks in surface-water catchments
- Willey JM, Sherwood LM, Woolverton CJ (2009) *Microbiología de Prescott*. Harley y Klein
- Wiszniowski J, Robert D, Surmacz-Gorska J, Miksch K, Malato S, Weber J-V (2004) Solar photocatalytic degradation of humic acids as a model of organic compounds of landfill leachate in pilot-plant experiments: influence of inorganic salts. *Appl Catal B Environ* 53(2):127–137
- Yang J-K, Lee S-M (2006) Removal of Cr(VI) and humic acid by using TiO₂ photocatalysis. *Chemosphere* 63(10):1677–1684
- Yuranova T, Enea O, Mielczarski E, Mielczarski J, Albers P, Kiwi J (2004) Fenton immobilized photo-assisted catalysis through a Fe/C structured fabric. *Appl Catal B Environ* 49(1):39–50

Publisher's note Springer Nature remains neutral with regard to jurisdictional claims in published maps and institutional affiliations.